# Microwave-Induced Polyol-Process Synthesis of Copper and Copper Oxide Nanocrystals with Controllable Morphology

Yu Zhao,[a] Jun-Jie Zhu,*[a] Jian-Min Hong,[a] Ningsheng Bian,[a] and Hong-Yuan Chen[a]

**Keywords:** Copper / Copper oxides / Microwaves / Nanostructures / UV / Vis spectroscopy

Different morphologies of copper and copper oxide nanocrystallites, including radially arrayed whiskers, cubic particles and sphere particles, have been successfully synthesized by a microwave-induced method under ambient conditions. In aqueous solution containing different ethylene glycol concentrations, copper acetate hydrate produces different reduction products. The as-prepared copper and copper oxide crystallites were characterized by various techniques, including X-ray powder diffraction, transmission electron microscopy, selected-area electron diffraction and UV/Vis absorption spectroscopy. It was found that microwave irradiation plays a critical role in the formation of the products; temperature was also found to be important in the reaction. The irradiation time and copper acetate concentration also affect the morphology of the products. The possible formation mechanism is also discussed.


## Introduction

Nanometer-sized metals, semiconductors, and oxides are of great interest because they can have physical and chemical properties that are not characteristic of the atoms or of their bulk counterparts. The large surface area to volume ratio can contribute to some of the unique properties of nanoparticles.[1−5] Among them, Cu, $Cu_2O$ and CuO are industrially important materials that are widely used in fields such as magnetic storage media, solar energy transformation, electronics, sensors, catalysis, batteries, resonance imaging and so forth.[6−12] In the past, some successful attempts have been made to synthesize nanoparticles of copper and copper oxides, such as sonochemical methods,[13−15] microwave irradiation,[16] photochemical methods,[17−20] hydrothermal and solvothermal methods,[21,22] electrochemical methods,[23−31] sol-gel methods,[32−35] solid-state reactions,[36] chemical reduction and decomposition route[37−42] and so on.

Microwaves are a portion of the electromagnetic spectrum with frequencies in the range of 300 MHz to 300 GHz. The corresponding wavelengths of these frequencies are 1 m to 1 mm. The most commonly used frequency is 2.45 GHz. The degree of interaction of microwaves with a dielectric medium is related to the material′s dielectric constant and dielectric loss.[43] When microwaves penetrate and propagate through a dielectric solution or suspension, the internal electric fields generated within the affected volume induce translation motions of free or bound charges such as electrons or ions and rotate charged complexes such as dipoles.[43] The resistance of these induced motions due to inertial, elastic, and frictional force, which are frequency dependent, causes losses and attenuates the electric field. Compared to ultrasonic irradiation, there is no similar bubble formation during microwave heating, although superheating occurs in localized spots. The main advantages of microwave-assisted reactions over conventional methods in synthesis are: (a) the kinetics of the reaction are increased by one to two orders of magnitude, (b) novel phases are formed, (c) the initial heating is rapid, which can lead to energy savings, and (d) selective formation of one phase over another often occurs.[44−46] One possible hypothesis for these microwave-induced effects is the generation of localized high temperatures at the reaction sites to enhance reaction rates in an analogous manner to that of ultrasonic waves,[47] where both high temperatures and pressures have been reported during reactions. The enhanced kinetics of crystallization can lead to energy savings of up to 90%.[48]

The polyol method is a low-temperature process that is environmentally benign because the reactions are carried out under closed-system conditions. It was first introduced to produce metal submicron-sized powders.[49−51] In this method, a suitable solid metal salt is suspended in a liquid polyol. The suspension is stirred and heated to a certain temperature; the reduction of the starting compound yields fine metal powders. The polyol itself acts not only as a solvent in the process but also as a stabilizer, limiting particle growth and prohibiting agglomeration.[52−54] Recently, this method has also been extended to the preparation of metal oxides[55−57] and metal chalcogenides.[58−60] Tarascon and co-workers have demonstrated that in these reactions the

[a] State Key Laboratory of Coordination Chemistry, Department of Chemistry, Nanjing University, Nanjing, 210093, P. R. China
Supporting information for this article is available on the WWW under http://www.eurjic.org or from the author.

  DOI: 10.1002/ejic.200400258 

temperature is a dominant factor in affecting the reactivity. Three factors are influenced by the temperature: (1) the reduction potential of ethylene glycol, (2) the rupture and creation of chemical bonds, and (3) diffusion.[61] All these factors make microwave-heating techniques favorable for the fabrication of metal and metal oxides by using ethylene glycol as a solvent. The ethylene glycol is an excellent susceptor for the microwave radiation because of its high permanent dipole. The metallic particles produced as intermediates in the polyol reaction are also good for this purpose.

In this paper, we present a novel microwave-induced polyol route to synthesize different morphologies of Cu, $Cu_2O$ and CuO nanoparticles. Ethylene glycol (EG) aqueous solutions with different concentration were used in order to control the reaction temperature during the microwave heating. Cu, $Cu_2O$ or CuO were formed in the different conditions. The effect on the morphology of the nanoparticles was also investigated. It was found to be a fast, convenient, mild, energy efficient and environmentally friendly route to produce nanoparticles of Cu, $Cu_2O$ and CuO.

## Results and Discussion

In order to study the nature and morphology of the products, various techniques such as X-ray diffraction (XRD), transmission electron microscopy (TEM), selected-area electron diffraction (SAED) and UV/Vis absorption spectroscopy were employed.

The results of the powder XRD analysis are shown in Figure 1 (see a−e). The diffraction peaks correspond to the reflection of: (a) CuO (CCID file no. 801916 monoclinic), (b) CuO mixed with $Cu_2O$, (c) $Cu_2O$ (CCID file no. 782076 cubic), (d) $Cu_2O$ mixed with Cu, and (e) Cu (CCID file no. 040836 cubic). In all the reactions, highly crystalline products were obtained. The positions of the peaks are in good agreement with literature values.

TEM images of the products are presented in Figure 2 (see a−e), where the different morphologies that be achieved simply by changing the water/EG ratio of the solvent can be clearly observed. Figure 2 (a) depicts the morphology of CuO, which shows radially arrayed whiskers. In this image, a single whisker is calculated to be about 80 nm in length and less than 10 nm in diameter; the SAED pattern of the products is shown in the inset. Figure 2 (b) shows a mixture of whiskers and cubic particles. Two different phases can be observed clearly in this picture. According to the SEAD images, and compared with the other SEAD patterns shown in Figure 2 (see a and c), it can be concluded that the whiskers are CuO of monoclinic phase [SAED pattern inset top right in Figure 2 (b)], and the cubes are $Cu_2O$ in the cubic phase (SAED pattern inset bottom left). $Cu_2O$ particles are observed as shown in Figure 2 (c); they are around 50 nm cubic nanoparticles. The SAED pattern of a single crystal of one of these particles is shown in the inset. Figure 2 (d) depicts Cu mixed with $Cu_2O$ particles; the products are not clearly separated. We conclude it to be mixture only by the XRD pattern in Figure 1. Figure 2 (e) depicts Cu particles, the size of which ranges from 100−120 nm. The SEAD pattern of these copper particles is inset.

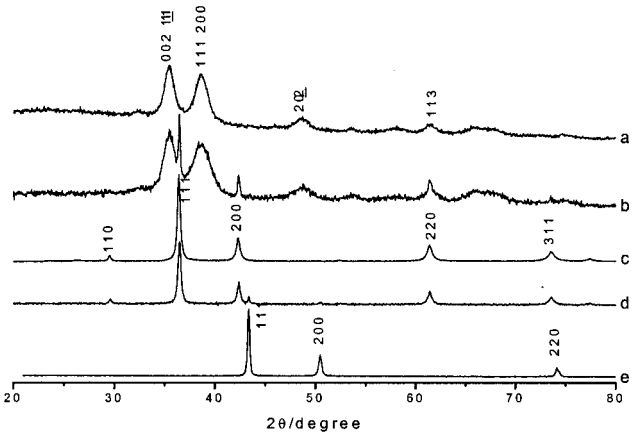


Figure 1. XRD patterns of: (a) CuO; (b) CuO mixed with $Cu_2O$; (c) $Cu_2O$; (d) $Cu_2O$ mixed with Cu; (e) Cu

In order to elucidate the mechanism of temperature control in the EG aqueous solution, we first supposed that the ethylene glycol and water mixture is an ideal binary system, which therefore behaves according to Raoults Law

$$y_A = x_A \cdot P^*_A / P$$

with $y_A$ = mol fraction of substance A in the vapor phase equilibrium with the solution, $X_A$ = mol fraction of substance A in the solution; $P^*_A$ = equilibrium vapor pressure of substance A; $P$ = vapor pressure of the whole system.

We calculated the theoretical boiling point of the system at different water volume ratios; the results are depicted in Figure 3. In our microwave dielectric heating process, the system temperature elevates rapidly. The reaction temperatures measured fit well with the theoretical values. As a result, an accurate and average temperature can be controlled in our microwave dielectric heating system.

As far as we know, when the solvent is pure ethylene glycol copper acetate is only partly dissolved and no chemical reaction occurs at 108 °C; when the solvent is water, copper acetate is completely soluble. On the contrary, in the EG aqueous solution, when the reaction temperature varies between 90 and 108 °C, CuO can be produced. We propose the process of producing CuO as follows: first, copper acetate hydrate dissolves in the solution; then EG esterifies with $OAc^-$ to produce ethylene glycol monoacetate and $OH^-$; finally $OH^-$ and $Cu^{2+}$ ion combine in solution and then dehydrate to form CuO. The reaction can be schematized as follows:

$$CH_3COO^- + HOCH_2CH_2OH \xrightarrow{\Delta} CH_3COOCH_2CH_2OH + OH^- \quad (1)$$

$$Cu^{2+} + 2\,OH^- \xrightarrow{\Delta} CuO\,(s) + H_2O \quad (2)$$

  

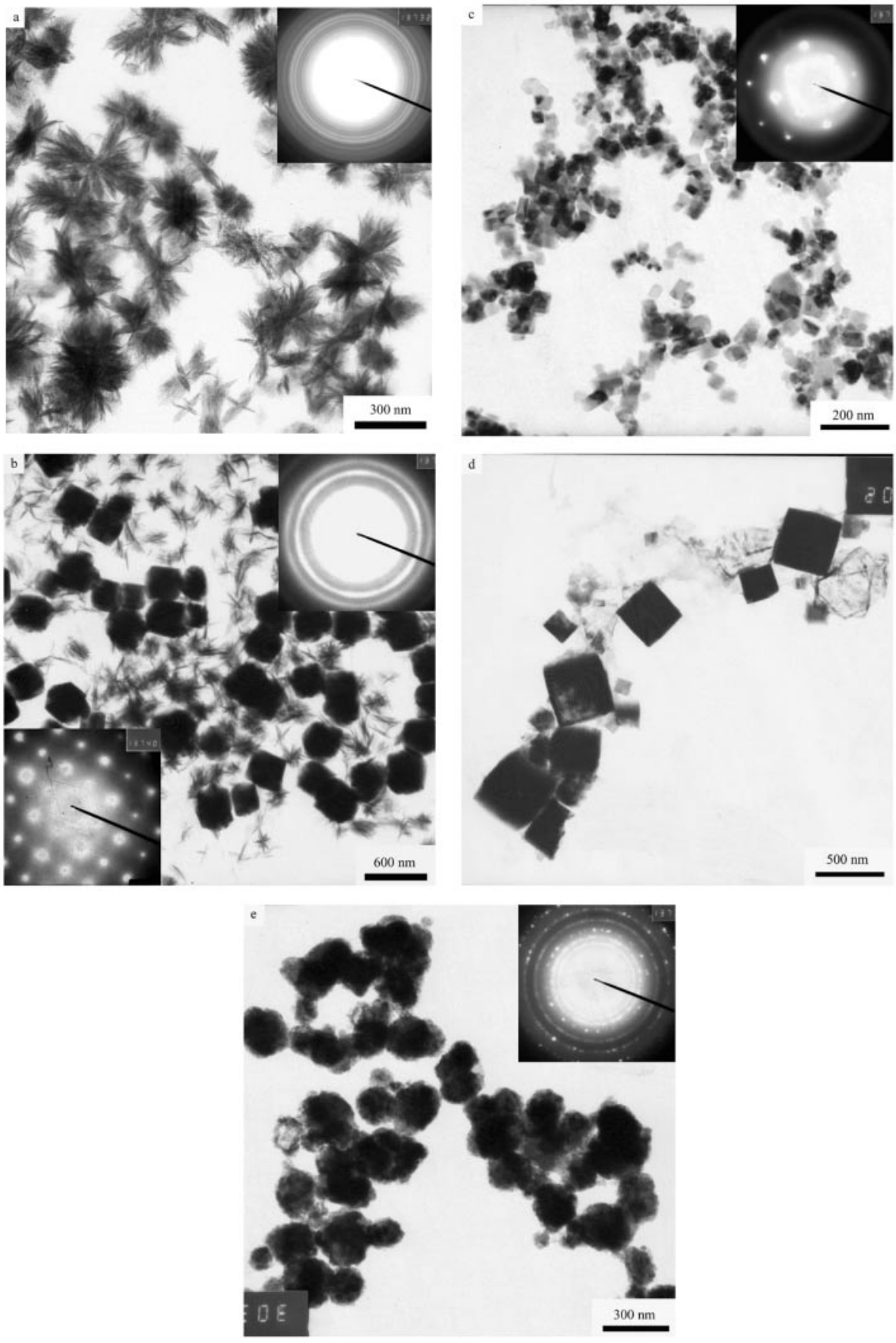


Figure 2. The TEM images of as-prepared: (a) CuO (inset: SEAD of CuO); (b) CuO mixed with $Cu_2O$ (inset bottom left: SAED of the whiskers; top right: SAED of a single cube); (c) $Cu_2O$ (inset: SEAD pattern of $Cu_2O$) (d) $Cu_2O$ mixed with Cu; (e) Cu (inset: SAED pattern of Cu particles)

  

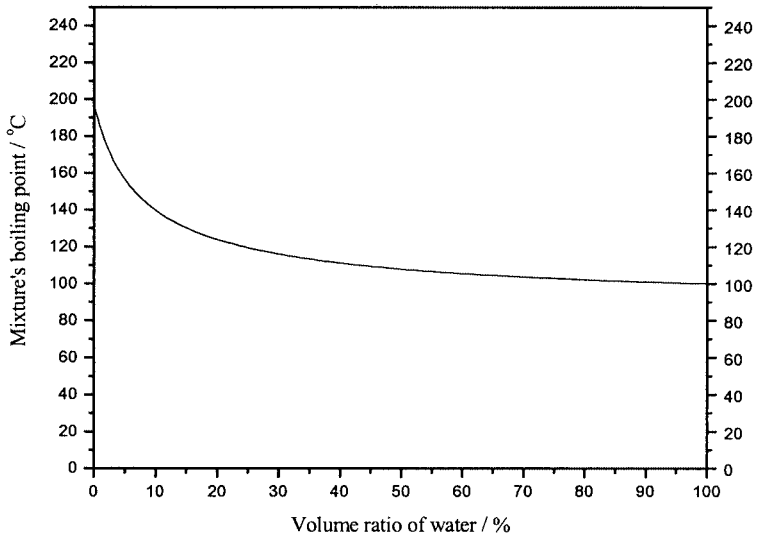


Figure 3. Theoretical boiling points with different EG volume ratios in the EG aqueous system

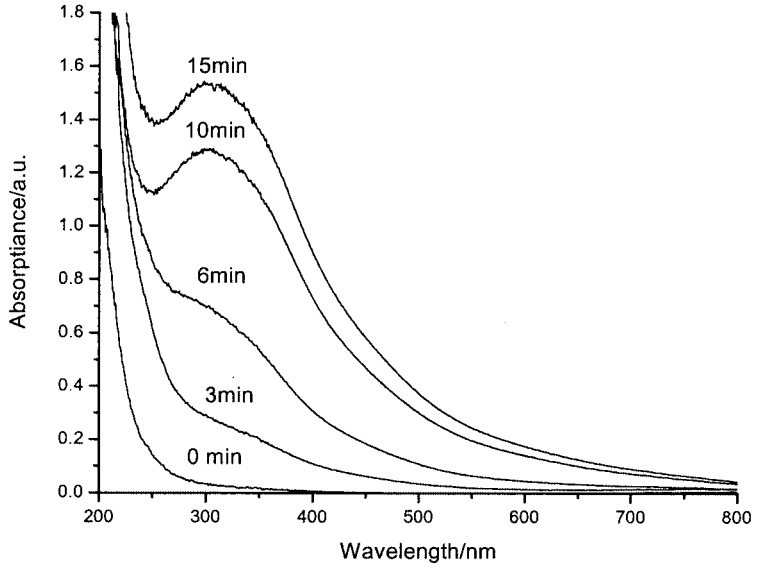


Figure 4. The UV/Vis absorption spectra of a suspension of copper acetate (0.03 g/40 mL) suspended in 49% EG aqueous solution after different microwave irradiation times; the numbers on the spectra indicate the time of irradiation; path length = 1 cm

To prove the reaction mechanism, we removed the water from the solvent for GC-MS detection after removing the precipitate by centrifugation. The results show that ethylene glycol monoacetate is the only reaction product remaining in solution.

To demonstrate the formation process of CuO nanocrystals, we recorded UV/Vis absorption spectra at different reaction times (Figure 4). There is no absorption present at the beginning of the reaction (0 min). As the reaction proceeds, however, an absorption shoulder appears at around 310 nm. After 15 minutes irradiation, the suspension becomes dark-brown, and a broad absorption peak centered at 310 nm can be observed. There is no obvious shift of the absorption peak with time. This means that the crystal size changes very little during the whole precipitation process. As an ionic reaction, reaction 2 is comparatively fast, so the formation of CuO nanocrystals is determined by reaction 1. In this process, the single whiskers prepared from different copper acetate concentration have the same size.

Figure 5 (see a−d) shows the change in morphology of as-prepared CuO as a function of time. The growth of CuO-whisker arrays can be described by three steps. First, crystal seeds of CuO are formed. These seeds then grown into whiskers, and, in the end, the CuO whiskers assemble into radially arrayed whiskers.

The concentration of copper acetate also plays a dramatic role in determining the morphology (Figure 6). In the case of a single whisker of the CuO nanocrystals, the crystal size is almost the same for all copper acetate concentration, but the morphology varies: the higher the concentration is, the denser the radial arrays will be. As we can see, when the

  

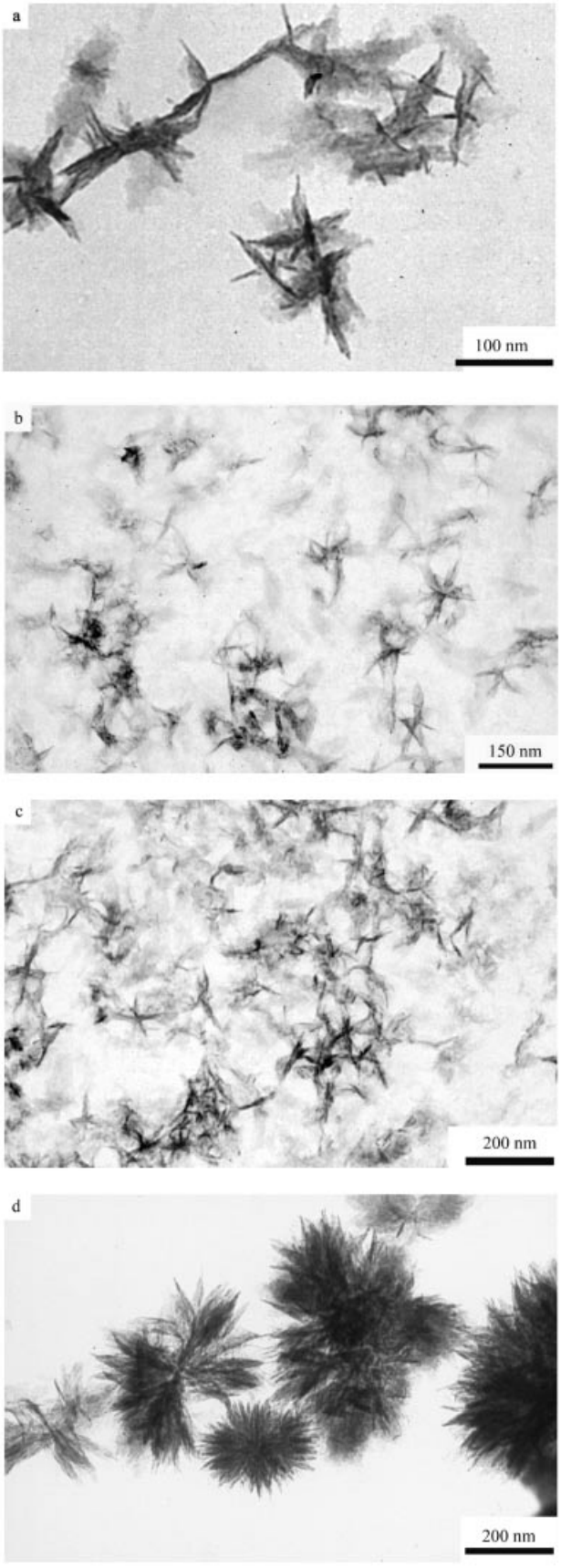


Figure 5. TEM images of CuO as a function of reaction time: a) 3 min; b) 6 min; c) 10 min; d) 15 min (0.03 g/40 mL copper acetate in 49% EG aqueous solution)

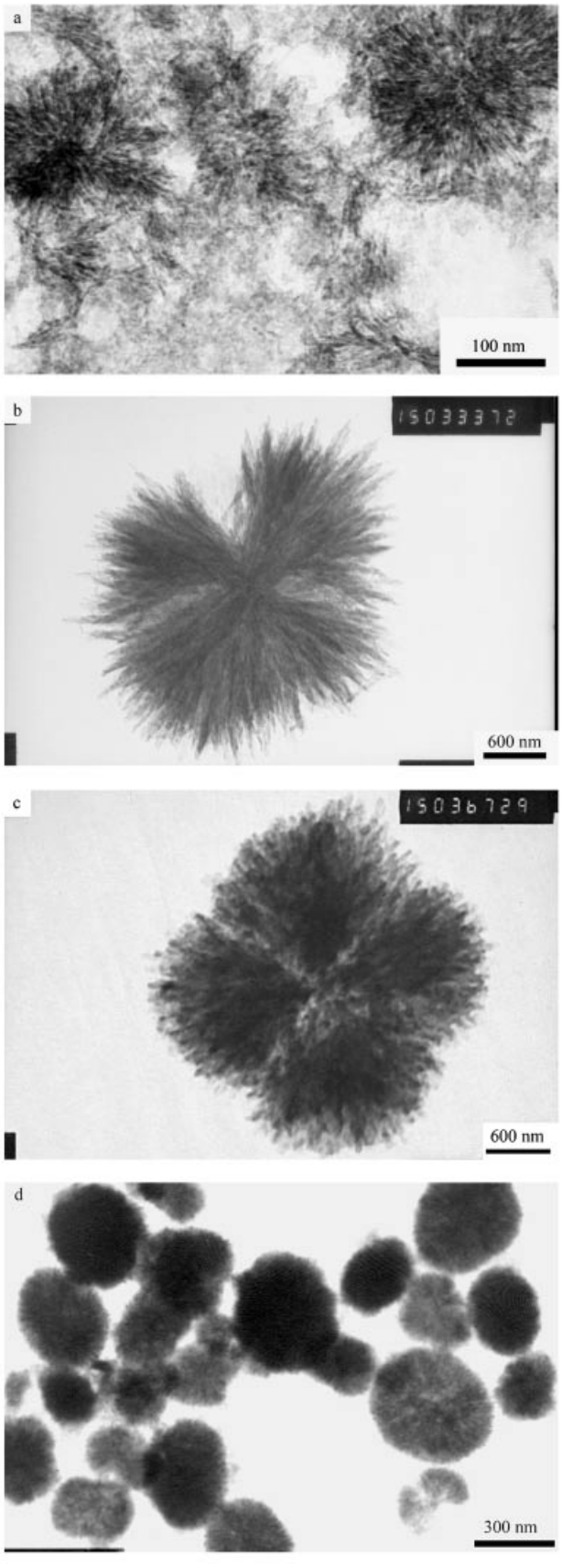


Figure 6. TEM images of CuO at various copper acetate concentrations: a) 0.03 g; b) 0.30 g; c) 0.70 g; d) 1.00 g (in 40 mL 49% EG aqueous solution)

  

copper acetate concentration increases to 0.70 g/40 mL, the CuO radical arrays are so dense that they look like a sphere (see d in Figure 6). Interestingly we also found that the growth of the radial whisker arrays is directed mainly along the axes of a tetrahedron.

Cu and $Cu_2O$ nanocrystals can also be prepared by this method; they follow a reduction mechanism. At 197 °C, the reduction product is Cu. Fievet et al.[2] have proposed that the metal particles are formed by nucleation and growth from the solution. According to this mechanism, we have proposed a formation process for the Cu nanoparticles: first, under dielectric heating, copper acetate hydrate dissolves completely in ethylene glycol, and then the intermediate solid phase between the starting material and the final metal powder is formed; during the second stage of the reaction the re-dissolution of the intermediate solid phase takes place. The reduction action of ethylene glycol is due to diacetyl, which is formed by a duplicative oxidation of acetaldehyde previously produced by dehydration of ethylene glycol.

The reaction can be schematized as follows:

$$2\ CH_2OH\text{-}CH_2OH \xrightarrow{-H_2O} 2\ CH_3CHO$$

Intermediate phase

$$\longrightarrow CH_3\text{-}CO\text{-}CO\text{-}CH_3 + H_2O + 2\ Cu$$

UV/Vis spectra were taken as a function of time (Figure 7). After six minutes irradiation, an absorption shoulder appears at around 490 nm, which indicates an intermediate phase. The phase will be shown to be $Cu_2O$ later. After nine minutes, colloidal copper has formed with an absorption peak at 580 nm. This absorption can be attributed to the plasma resonance absorption of the copper particles. As the reaction progresses, the copper colloid aggregates and precipitates. As a result, after 15 minutes the absorption peak at 580 nm has almost disappeared.

Figure 8 (a−d) depict the change in morphology of copper as a function of time. After six minutes, $Cu_2O$ cubic particles of about 300 nm have formed. This $Cu_2O$ is continuously being reduced to give dispersedCu particles with a dispersed particle size of about 15 nm in diameter (c in Figure 8). However, after reaction for 15 minutes, the Cu aggregates into particles of about 60 nm.

$Cu_2O$ is obtained at 140 °C. UV/Vis absorption spectra were recorded after different reaction times to investigate the reaction (Figure 9). Only after 12 minutes did the absorption shoulder at around 460 nm appear. This peak can be attributed to $Cu_2O$, and corresponds well with the absorption band of the intermediate phase in the preparation of Cu nanoparticles.

The growth of $Cu_2O$ nanoparticles was also investigated (Figure 10). As can be seen from the morphology of $Cu_2O$ after different reaction times, the $Cu_2O$ is formed as cubes of about 40 nm (Figure 10, a). As the reaction proceeds the particles grow further. It is interesting that hexagons [Figure 10 (d)] and truncated cubes [Figure 10 (e)] are also found in the reaction products; they can be regarded as intermediate morphologies en route to cubic particles. An SEAD pattern was also measured. As calculated, the inserted SEAD pattern of a truncated cube in Figure 10 (d) shows the (001) face and the hexagon in Figure 10 (e) shows the (111) face; they are both $Cu_2O$ of primitive cubic phase. As the reaction time is prolonged to 30 minutes, we can get cubic $Cu_2O$ as large as 500 nm. It is therefore possible to control the size of the $Cu_2O$ crystals.

## Conclusion

Using a novel microwave-induced polyol process, we have successfully synthesized copper, cuprites and copper(II) oxides systematically. The EG aqueous solution was heated by microwave irradiation, easy and precise control on the temperature was realized. By varying the conditions we

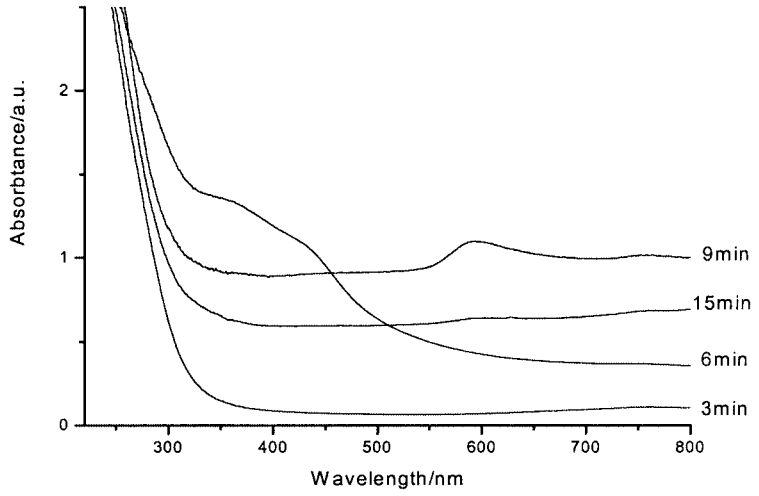


Figure 7. The UV/Vis absorption spectra of a suspension of copper acetate (0.03 g/40 mL) in pure EG solution as a function of irradiation time; the numbers on the spectra indicate the time of irradiation; path length = 1 cm

  

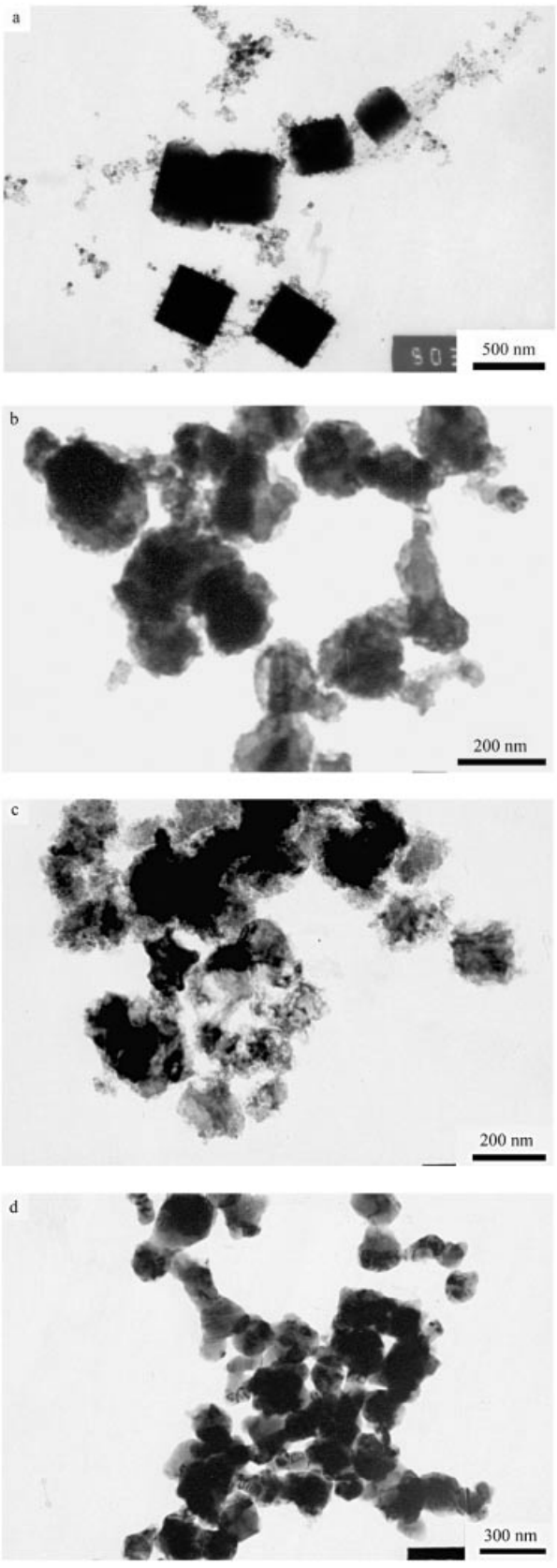


Figure 8. The TEM images in the formation of Cu as a function of reaction time: a) 6 min; b) 8 min; c) 9 min; d) 15 min (0.03 g/40 mL copper acetate in pure EG solution)

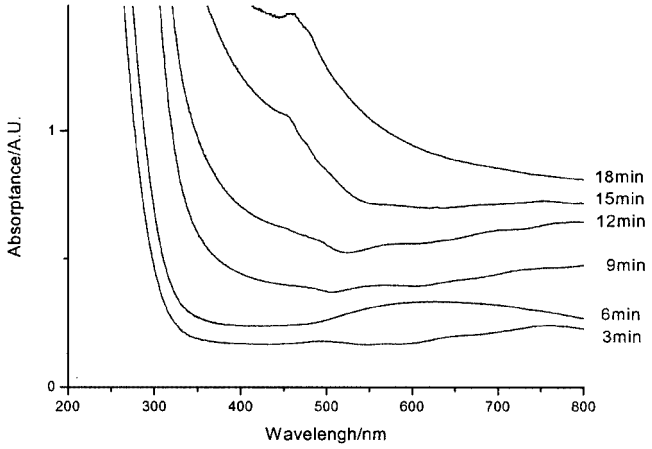


Figure 9. The UV/Vis absorption spectra of a suspension of copper acetate (0.03 g/40 mL) in 90% EG aqueous solution after different irradiation times; the numbers on the spectra indicate the irradiation time; path length = 1 cm

were able to prepare products with different morphology and particle sizes. A formation mechanism of the as-prepared products was proposed and the effects on the morphology and size were investigated. This kind of method is advantageous as it is a one-step reaction that occurs at relatively mild temperatures and gives well-dispersed products. Its extension to the preparation of other materials is currently being investigated.

## Experimental Section

**General:** All the experiments were performed in a modified National frequency-convertible microwave oven (NN-S570MFS). A reflux system was connected to the microwave oven. X-ray powder diffraction (XRD) measurements were performed on a Philips X′pert X-ray diffractometer at a scanning step of 0.03°, continue time 10 seconds, in the 2q range from 20° to 80°, with graphite monochromated Cu-$K_a$ radiation ($l$ = 0.15418 nm) and a nickel filter. Transmission electron microscopy (TEM) images and selected-area electron diffraction (SAED) images were recorded on a JEOL-JEM 200CX transmission electron microscope, at an accelerating voltage of 200 kV. The samples used for TEM observations were prepared by dispersing some products in ethanol followed by ultrasonic vibration for 30 min, then placing a drop of the dispersion onto a copper grid coated with a layer of amorphous carbon. A Shimazu UV-2401PC photospectrometer was used to record the UV/Vis absorption spectra of the as-prepared samples dispersed in water.

**Synthesis of Copper and Copper Oxides:** In a typical procedure, the appropriate amount of $Cu(OAc)_2 \cdot H_2O$ was added into an 80 mL round-bottomed flask, and then 40 mL of EG aqueous solution was added into the same flask. The mixture was placed into the microwave reflux system and the reaction was carried out under ambient conditions for 15 minutes at a power of 365 W. The detailed reaction conditions in various EG aqueous solutions are listed in Table 1. The reactants dissolved in the EG aqueous solution after irradiating for 3 min. As the reaction progressed a large amount of precipitate formed (dark-brown for CuO, reddish yellow for $Cu_2O$, and red for Cu). After the reaction, the suspension was

  

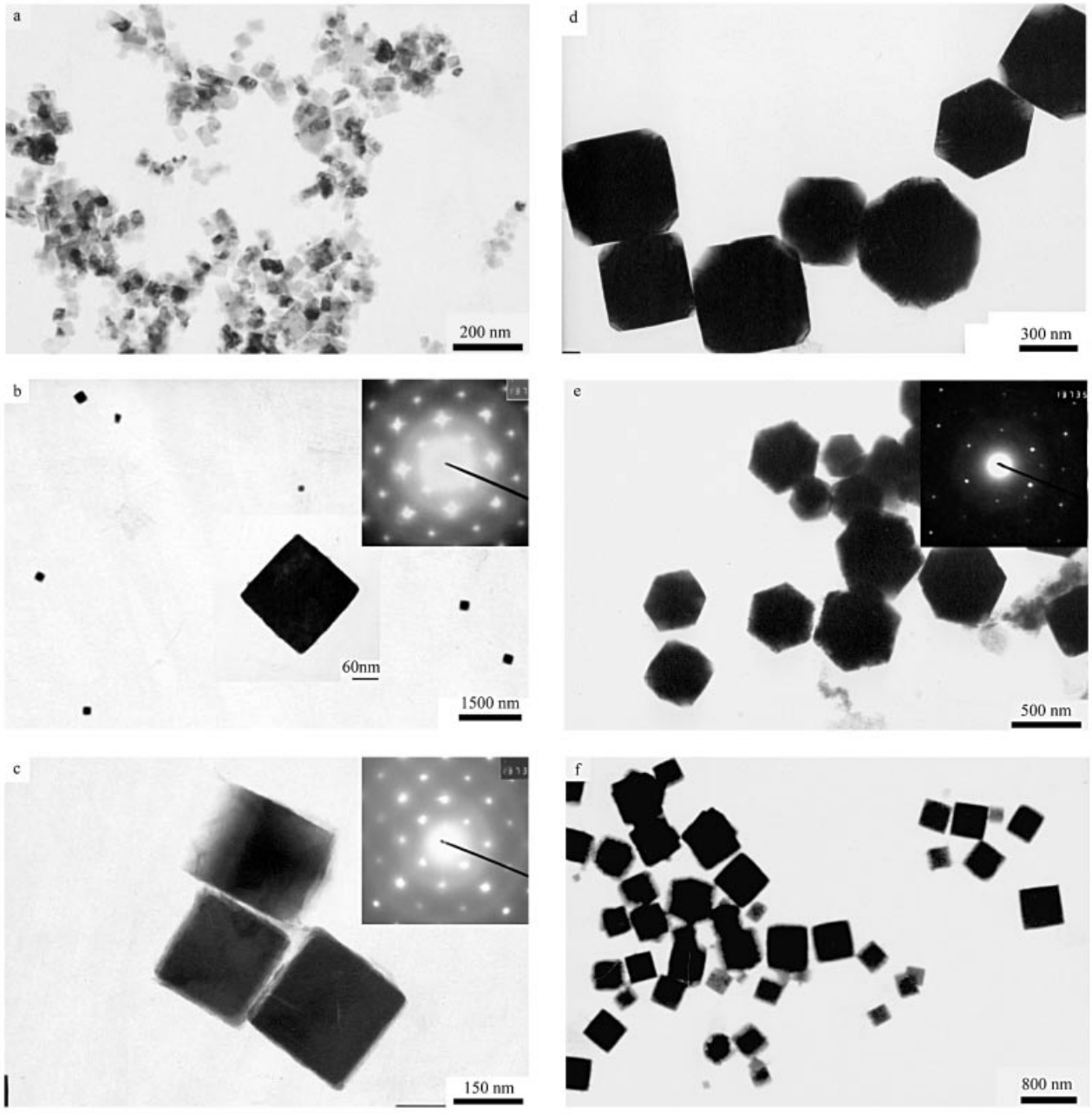


Figure 10. The TEM images of $Cu_2O$ as a function of reaction time: a) 3 min; b) 6 min; c) 9 min; d) and e) 15 min; f) 30 min (0.03 g/40 mL copper acetate in 90% EG aqueous solution)

Table 1. The reaction conditions in various EG aqueous solutions and products via Microwave dielectric heating

| Condition | EG volume ratio (%) | Water volume ratio (%) | Reaction temp. (°C) | Precipitate |
|---|---|---|---|---|
| o | 0 | 100 | 100 | – |
| a | 49 | 51 | 108 | CuO |
| b | 75 | 25 | 119 | CuO and $Cu_2O$ |
| c | 90 | 10 | 140 | $Cu_2O$ |
| d | 95 | 5 | 156 | $Cu_2O$ and Cu |
| e | 100 | 0 | 197 | Cu |

cooled to room temperature and the precipitate was centrifuged, washed with distilled water, absolute ethanol and acetone in sequence and dried in vacuo at room temperature. The final products were collected for characterizations. The products of the different reactions are also listed in Table 1.

## Acknowledgments

This work was supported by the National Natural Science Foundation of China (No.20325516, 90206037) and the Research Foundation for the Doctoral Program of the Ministry of Education of China (Grant No. 20020284022). The authors also thank Prof. Xinhua Xia and Mr. Zhengwei Shi for allowing us to use their facilities.

[1] M. D. Morse, *Chem. Rev.* **1986**, *86*, 1049−1109.
[2] W. P. Halperin, *Rev. Mod. Phys.* **1986**, *58*, 533−603.
[3] A. Henglein, *Chem. Rev.* **1989**, *89*, 1861−1873.

  

[4] G. D. Stucky, J. E. MacDougall, *Science* **1990**, *247*, 669−678.
[5] V. V. Kresin, *Phys. Rep.* **1992**, *220*, 1−52.
[6] A. Inoue, B. L. Shen, *J. Mater. Res.* **2003**, *18*, 2799−2806.
[7] S. Krongelb, L. T. Romankiw, J. A. Tornello, *IBM J. Res. Dev.* **1998**, *42*, 575−585.
[8] T. Mitsuyu, O. Yamakazi, K. Ohji, K. Wasa, *Ferroelectrics* **1982**, *42*, 233−240.
[9] M. M. Viitanen, W. P. A. Jansen, R. G. van Welzenis, H. H. Brongersma, D. S. Brands, E. K. Poels, A. Bliek, *J. Phys. Chem. B* **1999**, *103*, 6025−6029.
[10] U. Bjoerksten, J. Moser, M. Graetze, *Chem. Mater.* **1994**, *6*, 858−863.
[11] J. Tamaki, K. Shimanoe, Y. Yamada, Y. Yamamoto, N. Miura, N. Yamazoe, *Sens. Actuat. B* **1998**, *49*, 121−125.
[12] Y. Jiang, S. Decker, C. Mohs, K. J. Klabunde, *J. Catal.* **1998**, *180*, 24−35.
[13] R. V. Kumar, Y. Mastai, Y. Diamant, A. Gedanken, *Chem. Mater.* **2000**, *12*, 2301−2305.
[14] R. V. Kumar, Y. Mastai, Y. Diamant, A. Gedanken, *J. Mater. Chem.* **2001**, *11*, 1209−1213.
[15] N. A. Dhas, C. P. Raj, A. Gedanken, *Chem. Mater.* **1998**, *10*, 1446−1452.
[16] H. Wang, J. Z. Xu, J. J. Zhu, H. Y. Chen, *J. Cryst. Growth* **2002**, *244*, 88−94.
[17] G. G. Condorelli, L. L. Costanzo, I. L. Fragala, S. Giuffrida, G. Ventimiglia, *J. Mater. Chem.* **2003**, *13*, 2409−2411.
[18] S. Kapoor, T. Mukherjee, *Chem. Phys. Lett.* **2003**, *370*, 83−87.
[19] A. V. Loginov, V. V. Gorbunova, T. B. Boitsova, *J. Nanopart. Res.* **2002**, *4*, 193−205.
[20] T. B. Boitsova, A. V. Loginov, V. V. Gorbunova, *Russ. J. Appl. Chem.* **1997**, *70*, 1507−1512.
[21] Z. Liu, Y. Yang, J. Liang, Z. Hu, S. Li, S. Peng, Y. J. Qian, *J. Phys. Chem. B* **2003**, *107*, 12658−12661.
[22] S. J. Chen, X. T. Chen, Z. L. Xue, L. H. Li, X. Z. You, *J. Cryst. Growth* **2002**, *246*, 169−175.
[23] M. G. Shumsky, J. A. Switzer, *Chem. Mater.* **1999**, *11*, 2289−2291.
[24] J. K. Barton, A. A. Vertegel, E. W. Bohannan, J. A. Switzer, *Chem. Mater.* **2001**, *13*, 952−959.
[25] L. Huang, H. Wang, Z. Wang, A. Mitra, D. Zhao, Y. Yan, *Chem. Mater.* **2002**, *14*, 876−880.
[26] S. Kenane, L. Piraux, *J. Mater. Res.* **2002**, *17*, 401−406.
[27] M. E. T. Molares, V. Buschmann, D. Dobrev, R. Neumann, R. Scholz, I. U. Schuchert, J. Vetter, *Adv. Mater.* **2001**, *13*, 62−65.
[28] I. Enculescu, Z. Siwy, D. Dobrev, C. Trautmann, M. E. T. Molares, R. Neumann, K. Hjort, L. Westerberg, R. Spohr, *Appl. Phys. A, Mater. Sci. Process.* **2003**, *77*, 751−755.
[29] Y. Konishi, M. Motoyama, H. Matsushima, Y. Fukunaka, R. Ishii, Y. Ito, *J. Electroanal. Chem.* **2003**, *559*, 149−153.
[30] T. Gao, G. W. Meng, Y. W. Wang, S. H. Sun, L. Zhang, *J. Phys.: Condens. Matter* **2002**, *14*, 355−363.
[31] D. K. Sarkar, X. J. Zhou, A. Tannous, M. Louie, K. T. Leung, *Solid State Commun.* **2003**, *125*, 365−368.
[32] C. L. Kitchens, M. C. McLeod, C. B. Roberts, *J. Phys. Chem. B* **2003**, *107*, 11331−11338.
[33] L. Armelao, D. Barreca, M. Bertapelle, G. Bottaro, C. Sada, E. Tondello, *Thin Solid Films* **2003**, *442*, 48−52.
[34] J. C. S. Wu, I. H. Tseng, W. C. Chang, *J. Nanopart. Res.* **2001**, *3*, 113−118.
[35] M. Epifani, G. T. De, A. Licciulli, L. Vasanelli, *J. Mater. Chem.* **2001**, *11*, 3326−3332.
[36] W. H. Wang, Y. J. Zhan, G. H. Wang, *Chem. Commun.* **2001**, 727−728.
[37] M. Yang, J. J. Zhu, *J. Cryst. Growth* **2003**, *256*, 134−138.
[38] W. Wang, Z. Liu, Y. Liu, C. Xu, C. Zheng, G. Wang, *Appl. Phys. A, Mater. Sci. Process.* **2003**, *76*, 417−420.
[39] C. K. Xu, Y. K. Liu, G. D. Xu, G. H. Wang, *Mater. Res. Bull.* **2002**, *37*, 2365−2372.
[40] W. Z. Wang, G. H. Wang, X. S. Wang, Y. J. Zhan, Y. K. Liu, C. L. Zheng, *Adv. Mater.* **2002**, *14*, 67−69.
[41] L. F. Gou, C. J. Murphy, *Nano. Lett.* **2003**, *3*, 231−234.
[42] M. H. Cao, C. W. Hu, Y. H. Wang, Y. H. Guo, C. X. Guo, E. B. Wang, *Chem. Commun.* **2003**, 1884−1885.
[43] W. H. Sutton, *Am. Ceram. Soc. Bull.* **1989**, *68*, 376.
[44] H. Katsuki, S. Komarneni, *J. Am. Ceram. Soc.* **2001**, *84*, 2313−2317.
[45] S. Komarneni, R. Roy, Q. H. Li, *Mater. Res. Bull.* **1992**, *27*, 1393−1405.
[46] S. Komarneni, *Ionics* **1995**, *21*, 95.
[47] K. S. Suslick, *Science* **1990**, *247*, 1439−1445.
[48] Brochure on AultraCLAVE by Milestone, Microwave Laboratory Systems (Monroe, CT).
[49] M. Figlarz, F. Fievet, J. P. Lagier, Europe patent no. 0113281; USA no. 4539041; Japan: application no. 24303783, **1985**.
[50] F. Fievet, J. P. Lagier, B. Bin, *Solid State Ionics* **1989**, *32*, 198−205.
[51] C. Feldmann, *Adv. Funct. Mater.* **2003**, *13*, 101−107.
[52] Y. G. Sun, Y. N. Xia, *Adv. Mater.* **2002**, *14*, 833−837.
[53] S. Komarneni, D. Li, B. Newalkar, H. Katsuki, A. S. Bhalla, *Langmuir* **2002**, *18*, 5959−5962.
[54] C. Feldmann, H. O. Jungk, *Angew. Chem. Int. Ed.* **2001**, *40*, 359−362.
[55] O. Palchik, J. J. Zhu, A. Gedanken, *J. Mater. Chem.* **2000**, *10*, 1251−1254.
[56] T. Yamamoto, Y. Wada, H. B. Yin, T. Sakata, H. Mori, S. Yanagida, *Chem. Lett.* **2002**, *10*, 964−965.
[57] F. Kooli, V. Rives, W. Jones, *Chem. Mater.* **1997**, *9*, 2231−2235.
[58] R. Harpeness, O. Palchik, A. Gedanken, V. Palchik, S. Amiel, M. A. Slifkin, A. M. Weiss, *Chem. Mater.* **2002**, *14*, 2094−2102.
[59] H. Grisaru, O. Palchik, A. Gedanken, M. A. Slifkin, A. M. Weiss, V. Palchik, *Inorg. Chem.* **2003**, *42*, 7148−7155.
[60] H. Grisaru, O. Palchik, A. Gedanken, V. Palchik, M. A. Slifkin, A. M. Weiss, Y. R. Hacohen, *Inorg. Chem.* **2001**, *40*, 4814−4815.
[61] F. Bonet, C. Guery, D. Guyromard, R. Herrera Urbina, K. Tekaia-Elhsissen, J. M. Tarascon, *Int. J. Inorg. Mater.* **1999**, *1*, 47−51.

Received March 30, 2004
Early View Article
Published Online August 26, 2004

  